Quantum Circuits and their Optical Implementations

Abraham Tibebu Asfaw

A Thesis
Presented to the Faculty
of Manhattan College
in Candidacy for the Degree
of Bachelor of Science

Recommended for Acceptance
by the Departments of
Electrical and Computer Engineering
and Physics
Advisers: Professor Bruce Liby
Professor Chester Nisteruk

May 2012

Abstract

Starting with Richard Feynman's suggestion that quantum mechanical computers may be able to efficiently simulate quantum mechanical systems [1], there has been a tremendous amount of effort worldwide to create scalable quantum computers. Various experts have analyzed possible implementation schemes for quantum computers. Much like the time when classical computers had several proposed schemes, quantum computers have seen many attractive candidates for their implementation.

Here, we introduce quantum architecture via quantum gates and circuits that result from their combinations. We investigate the mathematical models of these quantum gates and discuss the requirements for scalable quantum circuits. We find universal sets of logic gates that we then implement using optical devices that are commonly available in a laboratory setting. In doing so, we develop the analytical skills necessary for determining the feasibility of quantum architecture schemes.

Finally, we discuss the drawbacks of the single photon quantum computing scheme and discuss possible areas of research using this scheme.

Acknowledgements

The Manhattan College community has welcomed me with open arms and provided an environment where I was able to discover my academic interests. For this, I am very grateful for this, and for all the support given to me by my friends.

My attendance at Manhattan College would not have been possible without the generosity of Mr. and Mrs. O'Malley, to whom I am forever indebted.

As the first engineer in my family, I relied heavily on advice from all the professors in the Department of Electrical and Computer Engineering at Manhattan College. They have gone beyond providing academic mentorship to nurture my varying interests. In particular, Prof. Nisteruk has witnessed my interests as they changed from signals and systems to linear systems, and finally to quantum computing. I am grateful to him for encouraging me to work outside my comfort levels until I had something to be proud of. His frequent lessons of quantum mechanics outside my regular academic coursework have broadened my perspectives beyond the principles of electrical engineering.

Despite my major, I have always received support from the Department of Mathematics and Computer Science. Several professors in the department took the time to give me independent study courses. I am thankful to Prof. Bishop, Prof. Boothe, Prof. Goldstone, Prof. Jura and Prof. McCabe for their patience and support. In particular, Prof. Bishop and Prof. Boothe have nurtured my interest in mathematics and computer science through two rewarding research projects that have helped shape my career significantly.

I also want to acknowledge the support provided to me by the Department of Physics, and particularly by Prof. Liby. He took on the role of advising me willingly and filled the gaps in my knowledge of physical optics. His mentorship has prepared me well for my upcoming graduate studies.

I would like to thank my entire family for their continued support. My academic growth has always been supplemented by their wisdom. In particular, I would like to thank my brother Kidus for constantly reviewing anything I sent his way and my mother Hiwot for the emotional support that she has given me throughout my life at and away from home.

I would also like to thank my girlfriend Mahlet for being a constant source of motivation and encouragement.

Last but certainly not least, I would like to thank God for creating me and allowing me to delve into an exploration of the computing capabilities of quantum phenomena afforded by nature.

To R.P. Feynman, whose remarkable imagination brought the world's attention to quantum computers

Contents

List of Figures

Chapter 1

Quantum circuits

Classical computers use bits to represent information for computation. A bit can take on only one value at a time from a choice of two permitted values. For example, a bit 1 may be used to encode the information "turned on" while the bit 0 may be used to represent "turned off." A string of bits can be used to represent large chunks of information for computation. The study of computer architecture begins with a bottom-up approach in which bits are studied first, followed by bit operations leading to more complicated circuitry for manipulating bits. We follow a similar approach here. We will explain the most fundamental components of a quantum computer starting with the most basic element, the qubit.

1.1 The qubit

Qubits are the most fundamental elements of a quantum computer. They correspond to their classical computer counterparts known as bits. The most important difference between qubits and classical bits is the idea of quantum superposition – while a bit is limited to two values (say 0 and 1), a qubit can be in a state that consists of some "mixture" of either 0 and 1.

The most popular notation for a qubit is through the use of bras and kets following Dirac notation [4]. In this way, the wave function of a qubit is given by

$$|\psi\rangle = \alpha|0\rangle + \beta|1\rangle \tag{1.1}$$

where $|0\rangle$ and $|1\rangle$ are the *computational basis states*. These two states are essentially the quantum analogues of classical bits. In equation (1.1), α and β are complex numbers.

Classical bits can be measured for their information content without any effect on that information. A classical bit with a value of 1 can be measured to indicate this value. Following the measurement, the bit will remain in the same *state* as before measurement. A qubit differs from this significantly. Since the state of a qubit is described by a wave function as shown in (1.1), its measured value is predicted by quantum mechanics to be either $|0\rangle$ or $|1\rangle$ with probability $|\alpha|^2$ or $|\beta|^2$ respectively. For that reason, the coefficients α and β are the *probability amplitudes* of $|\psi\rangle$. Quantum

mechanics predicts that measurement will reveal state $|0\rangle$ with probability $|\alpha|^2$ and $|1\rangle$ with probability $|\beta|^2$ [8].

Despite this strange behavior of qubits, they exist in nature and can be implemented using several methods. For instance, in chapter 3 we realize qubits using photons. Active areas of research in qubit implementation study several schemes including ion traps, electron spins and NMR [16].

1.2 Bloch sphere interpretation of the qubit

We have discussed the meaning of the probability amplitudes in the qubit wave function defined in (1.1). Because the probabilities must sum to one, we have the following constraint.

$$|\alpha|^2 + |\beta|^2 = 1 \tag{1.2}$$

This results in a geometrical interpretation of the qubit. Because α and β are complex numbers, the wave function of a qubit may be rewritten as

$$|\psi\rangle = e^{i\gamma} \cos\frac{\theta}{2}|0\rangle + e^{i(\gamma+\varphi)} \sin\frac{\theta}{2}|1\rangle \tag{1.3}$$

$$= e^{i\gamma}\left(\cos\frac{\theta}{2}|0\rangle + e^{i\varphi}\sin\frac{\theta}{2}|1\rangle\right) \tag{1.4}$$

for some real numbers γ, θ and φ. Here, note that there is a global phase shift which produces no observable effects. We will ignore it and instead write the qubit as

$$|\psi\rangle = \cos\frac{\theta}{2}|0\rangle + e^{i\varphi}\sin\frac{\theta}{2}|1\rangle \tag{1.5}$$

This representation of a qubit results in a mapping with the unit sphere. The qubit in (1.5) is located at the point $(r = 1, \theta, \varphi)$ on the unit sphere in spherical coordinates. This unit sphere is named the *Bloch sphere* after the name of its originator. The Bloch sphere is an excellent way of visualizing single qubit states. It is shown in figure 1.1. Sadly, it cannot be used to visualize multiple qubit systems. However, in section 1.3, we introduce operations on single qubits and visualize the changes that they cause with the help of the Bloch sphere.

1.3 Single qubit operations

Operations on a qubit must preserve the norm of the qubit, i.e., given an operation O on a single qubit and two qubits $|\psi\rangle = a|0\rangle + b|1\rangle$ and $|\psi'\rangle = O|\psi\rangle = a'|0\rangle + b'|1\rangle$, the normalization conditions

$$a^2 + b^2 = a'^2 + b'^2 = 1 \tag{1.6}$$

must hold. For this reason, operators on single qubits are represented by 2x2 unitary matrices. A unitary matrix U has the defining property $U^\dagger U = UU^\dagger = I$ where $U^\dagger$
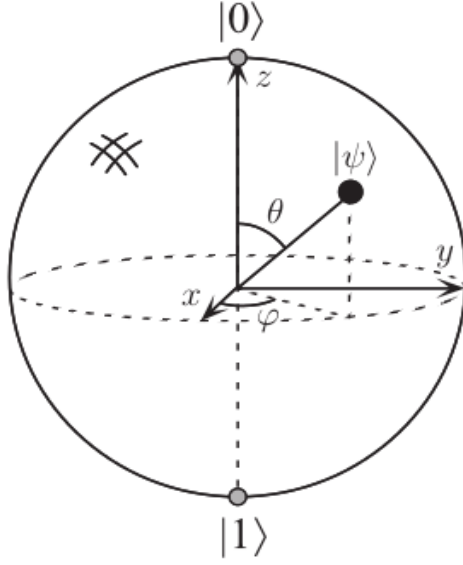
Figure 1.1: Bloch sphere interpretation of a qubit

is the adjoint of U. From this point on, we will refer to an operator by stating so explicitly or by giving its matrix representation.

A Hermitian operator is one that is self-adjoint. In other words, for a Hermitian operator H, $H^\dagger = H$. The most common single qubit operations are represented by the Pauli matrices. These special matrices are both Hermitian and unitary. Together with the identity matrix, they span the entire set of 2x2 matrices. In particular, they span all quantum mechanical observables which are represented as 2x2 Hermitian matrices [8]. The Pauli matrices are shown below.

$$X \equiv \begin{bmatrix} 0 & 1 \\ 1 & 0 \end{bmatrix} \ ; Y \equiv \begin{bmatrix} 0 & -i \\ i & 0 \end{bmatrix} \ ; Z \equiv \begin{bmatrix} 1 & 0 \\ 0 & -1 \end{bmatrix} \tag{1.7}$$

Three other operators that are commonly used in quantum computing are the Hadamard (H), $\pi/8$ (T) and phase (S) gates. These are shown below.

$$H \equiv \frac{X + Z}{\sqrt{2}} = \frac{1}{\sqrt{2}} \begin{bmatrix} 1 & 1 \\ 1 & -1 \end{bmatrix} \ ; T \equiv \begin{bmatrix} 1 & 0 \\ 0 & \exp(i\pi/4) \end{bmatrix} \ ; S \equiv T^2 = \begin{bmatrix} 1 & 0 \\ 0 & i \end{bmatrix} \tag{1.8}$$

Incidentally, the Hadamard gate is also known as the "square root of NOT" gate because it maps $|0\rangle$ to $(|0\rangle + |1\rangle)/\sqrt{2}$ and $|1\rangle$ to $(|0\rangle - |1\rangle)/\sqrt{2}$, both of which are "halfway" between $|0\rangle$ and $|1\rangle$. We can visualize the operation of the Hadamard gate in two steps:

1. Rotate the qubit vector in the Bloch sphere about the y axis by 90° and

2. Rotate the new qubit vector in the Bloch sphere about the x axis by 180°

The final vector represents the output of the Hadamard gate.

3

An additional property of the Pauli matrices is that $X^2 = Y^2 = Z^2 = I$. In Appendix A, we show how to exponentiate such matrices. Using these results, we now introduce three additional unitary matrices known as *rotation matrices* corresponding to the Pauli matrices. These are shown below.

$$R_x(\theta) \equiv \exp\left(-i\theta X/2\right) = \cos\left(\frac{\theta}{2}\right)I - i\sin\left(\frac{\theta}{2}\right)X = \begin{bmatrix} \cos\frac{\theta}{2} & -i\sin\frac{\theta}{2} \\ -i\sin\frac{\theta}{2} & \cos\frac{\theta}{2} \end{bmatrix} \quad (1.9)$$

$$R_y(\theta) \equiv \exp\left(-i\theta Y/2\right) = \cos\left(\frac{\theta}{2}\right)I - i\sin\left(\frac{\theta}{2}\right)Y = \begin{bmatrix} \cos\frac{\theta}{2} & -\sin\frac{\theta}{2} \\ \sin\frac{\theta}{2} & \cos\frac{\theta}{2} \end{bmatrix} \quad (1.10)$$

$$R_z(\theta) \equiv \exp\left(-i\theta Z/2\right) = \cos\left(\frac{\theta}{2}\right)I - i\sin\left(\frac{\theta}{2}\right)Z = \begin{bmatrix} \exp\left(-i\theta/2\right) & 0 \\ 0 & \exp\left(i\theta/2\right) \end{bmatrix} \quad (1.11)$$

In general, the rotation by θ about an axis defined by the real unit vector $\hat{n} = (n_x, n_y, n_z)$ is applied using the following matrix.

$$R_{\hat{n}}(\theta) \equiv \exp\left(-i\theta\frac{n_x X + n_y Y + n_z Z}{2}\right) = \cos\left(\frac{\theta}{2}\right)I - i\sin\left(\frac{\theta}{2}\right)(n_x X + n_y Y + n_z Z) \quad (1.12)$$

The rotation matrices R_x, R_y and R_z result in rotations about the x, y, and z axes respectively on the Bloch sphere.

We present a very useful way of representing unitary operator matrices below. Any unitary operator U can be represented by a matrix which is a product of rotations in the y and z axes plus a global phase. Appendix B proves this relation.

$$U = \exp\left(i\alpha\right) R_z(\beta) R_y(\gamma) R_z(\delta) \quad (1.13)$$

$$= e^{i\alpha} \begin{bmatrix} e^{-i\beta/2} & 0 \\ 0 & e^{i\beta/2} \end{bmatrix} \begin{bmatrix} \cos\frac{\gamma}{2} & -\sin\frac{\gamma}{2} \\ \sin\frac{\gamma}{2} & \cos\frac{\gamma}{2} \end{bmatrix} \begin{bmatrix} e^{-i\delta/2} & 0 \\ 0 & e^{i\delta/2} \end{bmatrix} \quad (1.14)$$

Yet another representation of a unitary operator matrix which follows from above is shown below.

$$U = \exp\left(i\alpha\right) AXBXC \quad (1.15)$$

The proof follows from (1.13) by making the following substitutions.

$$A \equiv R_z\left(\beta\right) R_y\left(\frac{\gamma}{2}\right) \quad (1.16)$$

$$B \equiv R_y\left(-\frac{\gamma}{2}\right) R_z\left(-\frac{\delta + \beta}{2}\right) \quad (1.17)$$

$$C \equiv R_z\left(\frac{\delta - \beta}{2}\right) \quad (1.18)$$

In the above representation, A, B and C are unitary themselves and $ABC = I$. These representations will be important as we define controlled operations using multiple qubits in the next section. One additional set of identities that we need to

Hadamard	$-\boxed{H}-$	$\dfrac{1}{\sqrt{2}}\begin{bmatrix} 1 & 1 \\ 1 & -1 \end{bmatrix}$
Pauli-X	$-\boxed{X}-$	$\begin{bmatrix} 0 & 1 \\ 1 & 0 \end{bmatrix}$
Pauli-Y	$-\boxed{Y}-$	$\begin{bmatrix} 0 & -i \\ i & 0 \end{bmatrix}$
Pauli-Z	$-\boxed{Z}-$	$\begin{bmatrix} 1 & 0 \\ 0 & -1 \end{bmatrix}$
Phase	$-\boxed{S}-$	$\begin{bmatrix} 1 & 0 \\ 0 & i \end{bmatrix}$
$\pi/8$	$-\boxed{T}-$	$\begin{bmatrix} 1 & 0 \\ 0 & e^{i\pi/4} \end{bmatrix}$

Figure 1.2: Single qubit gates and their circuit notations

keep in mind is the following. The proofs for these are straightforward substitutions and are not shown here.

$$HXH = Z \; ; \; HYH = -Y \; ; \; HZH = X \tag{1.19}$$

Figure 1.2 summarizes all the single qubit gates discussed above and shows their circuit notations.

1.4 Multiple qubits and controlled operations

So far, we have talked about operations on single qubits. We now discuss a class of operations on multiple qubits known as *controlled operations*. In particular, we will discuss two-qubit controlled operations. These discussions can intuitively be generalized for larger numbers of qubits.

1.4.1 Multiple qubits

Before discussing the operations, let us introduce the concept of multiple qubits. We introduced single qubits by discussing their classical counterparts. We saw that given the computational basis composed of two states, the general qubit wavefunction in (1.1) is a superposition of these states with the appropriate probability amplitudes. We will introduce multiple qubits in a similar fashion. Consider two classical qubits. They can be combined to form four classical possibilities: 00, 01, 10 and 11. Measurement will reveal one of these four possible states. Given two qubits, the wave

function of their combination is given by

$$|\psi\rangle = \alpha_{00}|00\rangle + \alpha_{01}|01\rangle + \alpha_{10}|10\rangle + \alpha_{11}|11\rangle \qquad (1.20)$$

such that

$$|\alpha_{00}|^2 + |\alpha_{01}|^2 + |\alpha_{10}|^2 + |\alpha_{11}|^2 = 1 \qquad (1.21)$$

Following measurement, the wave function will collapse to one of the four states with its respective probability.

Generally, given n qubits, there are 2^n states in the computational basis with 2^n corresponding probability amplitudes. Therefore, using 500 qubits, we can theoretically encode the states of all atoms in the universe!

1.4.2 Controlled operations

The simplest controlled operation is the controlled version of the classical NOT gate, known as the CNOT gate. It operates on two qubits known as the *control qubit* and the *target qubit*. Its operation is described as follows: if the control qubit is set (to $|1\rangle$), then the target qubit is inverted (from $|0\rangle$ to $|1\rangle$ and vice versa). The shorthand notation for the CNOT gate is given below.

$$\text{CNOT: } |control\rangle|target\rangle \to |control\rangle|control \oplus target\rangle \qquad (1.22)$$

The matrix representation for the CNOT operator can be determined as follows from the above shorthand notation.

$$\text{CNOT: } |0\rangle|0\rangle \to |0\rangle|0\rangle \qquad (1.23)$$
$$\text{CNOT: } |0\rangle|1\rangle \to |0\rangle|1\rangle \qquad (1.24)$$
$$\text{CNOT: } |1\rangle|0\rangle \to |1\rangle|1\rangle \qquad (1.25)$$
$$\text{CNOT: } |1\rangle|1\rangle \to |1\rangle|0\rangle \qquad (1.26)$$

In the computational basis $\{|0\rangle, |1\rangle\}$, the CNOT gate acts on two qubits and is therefore 4x4. The columns of the CNOT matrix are the outputs of $|0\rangle|0\rangle$, $|0\rangle|1\rangle$, $|1\rangle|0\rangle$ and $|1\rangle|1\rangle$ respectively. Hence,

$$\text{CNOT} \equiv \begin{bmatrix} 1 & 0 & 0 & 0 \\ 0 & 1 & 0 & 0 \\ 0 & 0 & 0 & 1 \\ 0 & 0 & 1 & 0 \end{bmatrix} \qquad (1.27)$$

The circuit notation for the CNOT operator is shown in figure 1.3. In general, a controlled-U operator can be represented by a matrix by noting how it affects combinations of input qubits. The shorthand notation is shown below.

$$\text{controlled-U: } |control\rangle|target\rangle \to |control\rangle U^{control}|target\rangle \qquad (1.28)$$
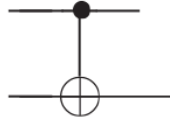
Figure 1.3: Circuit notation for a CNOT gate
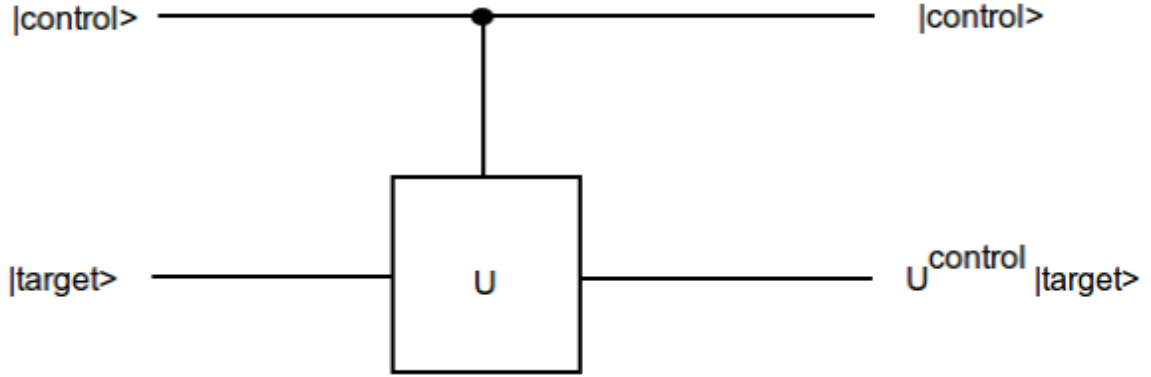
Figure 1.4: A controlled-U operator. Note the control and target qubits

This general notation leads to a general form for the matrix of a controlled-U operator, which is shown below.

$$\text{controlled-U} \equiv \begin{bmatrix} I & 0 \\ 0 & U \end{bmatrix} \tag{1.29}$$

Note that the above matrix is 4x4 because both I and U are 2x2. Also note that the CNOT operator has the same matrix representation as a controlled-X operator. Notationally,

$$\text{CNOT} \equiv \begin{bmatrix} 1 & 0 & 0 & 0 \\ 0 & 1 & 0 & 0 \\ 0 & 0 & 0 & 1 \\ 0 & 0 & 1 & 0 \end{bmatrix} = \begin{bmatrix} I & 0 \\ 0 & X \end{bmatrix} \tag{1.30}$$

The commonly used circuit notation for a controlled-U operation is shown in figure 1.4.

Recall from equation 1.15 that we can represent unitary operators by elementary operators. Therefore, for a controlled-U gate, we have the following: when the control is disabled, the identity matrix is applied to the target qubit. Otherwise,

Figure 1.5: A controlled-U gate decomposed into elementary single-qubit gates

$U = \exp(i\alpha) AXBXC$ is applied to the target qubit. Note the following.

$$\exp(i\alpha):\ |0\rangle|0\rangle \rightarrow |0\rangle|0\rangle \tag{1.31}$$

$$\exp(i\alpha):\ |0\rangle|1\rangle \rightarrow |0\rangle|1\rangle \tag{1.32}$$

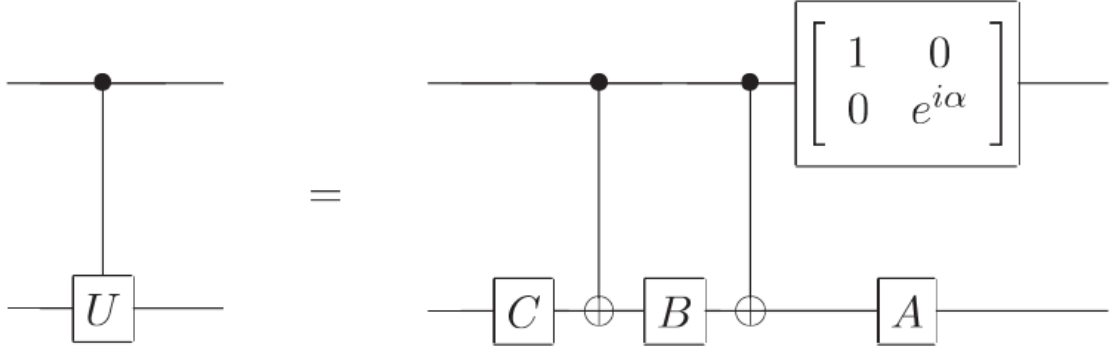$$\exp(i\alpha):\ |1\rangle|0\rangle \rightarrow |1\rangle\exp(i\alpha)\,(|0\rangle) = \exp(i\alpha)\,(|1\rangle)|0\rangle \tag{1.33}$$

$$\exp(i\alpha):\ |1\rangle|1\rangle \rightarrow |1\rangle\exp(i\alpha)\,(|1\rangle) = \exp(i\alpha)\,(|1\rangle)|1\rangle \tag{1.34}$$

From the above equations, we observe that the effect of the global phase can be applied to the control or target qubits. Since it only applies when the control qubit is set, we will apply it there, giving the circuit diagram in figure 1.5.

Also recalling the constraints on A, B and C such that $ABC = I$, this implies that the control qubit affects the X operators, turning them into CNOT gates.

The above discussion easily applies when there are multiple control and target qubits. Given a unitary operator U applied on n control qubits $\{x_1, x_2, \ldots, x_n\}$ and k target qubits $\{y_1, y_2, \ldots, y_k\}$, we have the following shorthand notation.

$$\text{controlled-U: } |x_1\rangle|x_2\rangle \ldots |x_{n-1}\rangle|x_n\rangle|y_1\rangle|y_2\rangle \ldots |y_{k-1}\rangle|y_k\rangle \rightarrow \tag{1.35}$$

$$|x_1\rangle|x_2\rangle \ldots |x_{n-1}\rangle|x_n\rangle U^{x_1 x_2 \ldots x_{n-1} x_n}|y_1\rangle|y_2\rangle \ldots |y_{k-1}\rangle|y_k\rangle \tag{1.36}$$

This shorthand notation is shown in circuit notation in figure 1.6.

1.5 Summary

In this chapter, we have introduced the two-state quantum system used in quantum computation known as the qubit. We have indicated its wave function and used the Bloch sphere as a means of visualizing qubits. The Bloch sphere is particularly important when we consider single qubit gates. It helps us visualize the effects of the unitary operators that we normally encounter in matrix form.
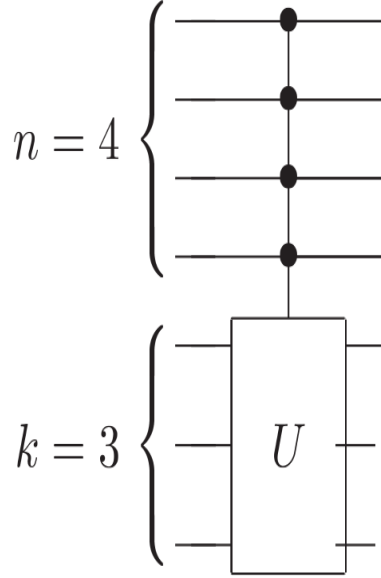
Figure 1.6: A multiple-control multiple-target controlled-U operator with 4 control and 3 target qubits

We have also discussed the fundamental single-qubit gates – the Pauli gates, their derived rotation operators, the Hadamard, phase and $\pi/8$ gates.

After introducing single-qubit gates, we showed how they can be controlled using additional qubits to form multiple-qubit gates. We showed how to derive the matrices corresponding to these operators and derived general controlled operations in terms of elementary single-qubit gates. The method of control was shown to be applicable even when the number of control and target qubits increases.

For additional reading, including topics such as universal gates and operator approximations, the interested reader is referred to chapter 4 of [16]. ∎

Chapter 2

Quantum mechanical analysis of the harmonic oscillator

2.1 Motivation

This chapter will provide the necessary background for understanding optical implementations of quantum gates. We introduce relevant operators such as annihilators and creators based on a quantum mechanical description of the harmonic oscillator. The material in this chapter is based on analysis of the harmonic oscillator provided in [7] and [8]. Additional material concerned with annihilators and creators can be found in [14].

2.2 Creation and annihilation operators

In linear algebra, the eigenvalues Ω and eigenvectors $|\Omega\rangle$ of an operator $\boldsymbol{O}$ are related as follows [18].

$$\boldsymbol{O}|\Omega\rangle = \Omega|\Omega\rangle \tag{2.1}$$

For real eigenvalues Ω, this essentially means that the effect of the operator $\boldsymbol{O}$ on its eigenvectors $|\Omega\rangle$ is scaling by a factor of Ω. For complex eigenvalues Ω, the eigenvector $|\Omega\rangle$ is scaled and rotated by the magnitude and phase angle of Ω respectively.

In quantum mechanics, physical observables are represented by Hermitian operators that have real eigenvalues [8, 18]. Recall that a Hermitian operator $\boldsymbol{H}$ has the property that $\boldsymbol{H}^\dagger = \boldsymbol{H}$. We represent operators with boldface symbols throughout the chapter. The Hamiltonian of a one-dimensional harmonic oscillator is given below.

$$\boldsymbol{H} = \frac{\boldsymbol{p}^2}{2m} + \frac{1}{2}K\boldsymbol{x}^2 \tag{2.2}$$

In addition, the commutator relationship $[\boldsymbol{x}, \boldsymbol{p}]$ relates the two physical observables in the above equation. The first term in the Hamiltonian is the kinetic energy, and the second is the potential energy. Thus, the Hamiltonian is the total energy of the

system [8]. The normalized position and momentum operators are

$$\boldsymbol{X} = \sqrt{\frac{K}{\hbar\omega_0}}\,\boldsymbol{x} \tag{2.3}$$

$$\boldsymbol{P} = \frac{\boldsymbol{p}}{\sqrt{m\hbar\omega_0}} \tag{2.4}$$

where $\omega_0 = \sqrt{\frac{K}{m}}$. The Hamiltonian expressed in terms of these normalized operators becomes

$$\boldsymbol{H} = \frac{\hbar\omega_0}{2}\left(\boldsymbol{P}^2 + \boldsymbol{X}^2\right) \tag{2.5}$$

with a new commutator relationship $[\boldsymbol{X}, \boldsymbol{P}] = j$. We introduce the non-Hermitian annihilator $\boldsymbol{a}$ and its adjoint $\boldsymbol{a}^\dagger$ as

$$\boldsymbol{a} = \frac{1}{\sqrt{2}}\left(\boldsymbol{X} + j\boldsymbol{P}\right) \tag{2.6}$$

$$\boldsymbol{a}^\dagger = \frac{1}{\sqrt{2}}\left(\boldsymbol{X} - j\boldsymbol{P}\right) \tag{2.7}$$

with a commutator $[\boldsymbol{a}, \boldsymbol{a}^\dagger] = 1$. We are also interested in the anti-commutator $\{\boldsymbol{a}, \boldsymbol{a}^\dagger\}$ of the annihilator and its adjoint. Note that

$$\boldsymbol{a}\boldsymbol{a}^\dagger = \frac{1}{2}\left(\boldsymbol{X}^2 + \boldsymbol{P}^2 + 1\right) \tag{2.8}$$

$$\boldsymbol{a}^\dagger\boldsymbol{a} = \frac{1}{2}\left(\boldsymbol{X}^2 + \boldsymbol{P}^2 - 1\right) \tag{2.9}$$

Hence, $\{\boldsymbol{a}, \boldsymbol{a}^\dagger\} = \boldsymbol{a}\boldsymbol{a}^\dagger + \boldsymbol{a}^\dagger\boldsymbol{a} = \boldsymbol{P}^2 + \boldsymbol{X}^2$. The Hamiltonian can now be expressed in terms of this anti-commutator.

$$\boldsymbol{H} = \frac{\hbar\omega_0}{2}\left(\boldsymbol{P}^2 + \boldsymbol{X}^2\right) = \frac{\hbar\omega_0}{2}\left(\boldsymbol{a}^\dagger\boldsymbol{a} + \boldsymbol{a}\boldsymbol{a}^\dagger\right) \tag{2.10}$$

$$= \hbar\omega_0\left(\boldsymbol{a}^\dagger\boldsymbol{a} + \frac{1}{2}\right) \tag{2.11}$$

We introduce an additional Hermitian operator known as the number operator $\boldsymbol{N}$ such that

$$\boldsymbol{N} = \boldsymbol{a}^\dagger\boldsymbol{a} \tag{2.12}$$

that counts the number of energy quanta excited in the harmonic oscillator. The eigenvectors $|n\rangle$ of $\boldsymbol{N}$ are known as *Fock* states and the corresponding eigenvalues are denoted as N_n such that

$$\boldsymbol{N}|n\rangle = N_n|n\rangle \tag{2.13}$$

Since $\boldsymbol{N}$ is Hermitian, it has orthonormal eigenvectors and real eigenvalues. In other words, for two eigenvectors $|n\rangle, |m\rangle$ of $\boldsymbol{N}$,

$$\langle m|n\rangle = \delta_{mn} \tag{2.14}$$

where

$$\delta_{mn} = \begin{cases} 1 & \text{if } m = n \\ 0 & \text{otherwise} \end{cases}$$

The annihilation operator and its adjoint have special effects on the Fock states [8].

$$\boldsymbol{a}|n\rangle = \sqrt{n}\,|n-1\rangle \tag{2.15}$$

$$\boldsymbol{a}^\dagger|n\rangle = \sqrt{n+1}\,|n+1\rangle \tag{2.16}$$

We define $\boldsymbol{a}|0\rangle = 0$ for the ground state of the harmonic oscillator. Note that the application of $\boldsymbol{a}$ leads to one less quantum while that of $\boldsymbol{a}^\dagger$ leads to an additional quantum. For this reason, the two operators are usually called the annihilation and creation operators respectively. Starting from the ground state, we can reach a Fock state $|n\rangle$ by repeated application of the creation operator followed by normalization.

$$|n\rangle = \frac{\boldsymbol{a}^\dagger|n-1\rangle}{\sqrt{n}} = \frac{\left(\boldsymbol{a}^\dagger\right)^2|n-2\rangle}{\sqrt{n}\sqrt{n-1}} = \ldots \tag{2.17}$$

$$= \frac{1}{\sqrt{(n)!}}\left(\boldsymbol{a}^\dagger\right)^n|0\rangle \tag{2.18}$$

Since the ground state has energy $\frac{\hbar\omega_0}{2}$ with each additional quantum contributing the same energy, the eigenvalues of the Hamiltonian of the harmonic oscillator are related to the Hamiltonian as

$$\boldsymbol{H}|n\rangle = E_n|n\rangle = \hbar\omega_0\left(n + \frac{1}{2}\right) \tag{2.19}$$

where E_n is the energy eigenvalue corresponding to the Fock state $|n\rangle$.

2.3 Matrix elements of the creation and annihilation operators

In this section, we will investigate the elements of the matrices that represent the annihilation and creation operators. From (2.6), we have

$$\boldsymbol{X} = \frac{1}{\sqrt{2}}\left(\boldsymbol{a}^\dagger + \boldsymbol{a}\right) \tag{2.20}$$

$$\boldsymbol{P} = \frac{j}{\sqrt{2}}\left(\boldsymbol{a}^\dagger - \boldsymbol{a}\right) \tag{2.21}$$

For Fock states $|m\rangle$ and $|n\rangle$, we now derive a series of relations that reveal the matrix elements of the annihilation and creation operators. Note that for an operator $\boldsymbol{O}$, $\langle m|\boldsymbol{O}|n\rangle$ is the element O_{mn} of the matrix representation of $\boldsymbol{O}$.

$$\langle m|\boldsymbol{a}|n\rangle = \sqrt{n}\,\langle m|n-1\rangle = \sqrt{n}\,\delta_{m,n-1} \qquad (2.22)$$

$$\langle m|\boldsymbol{a}^\dagger|n\rangle = \sqrt{n+1}\,\langle m|n+1\rangle = \sqrt{n+1}\,\delta_{m,n+1} \qquad (2.23)$$

$$\langle m|\boldsymbol{a}^\dagger\boldsymbol{a}|n\rangle = n\langle m|n\rangle = n\delta_{m,n} \qquad (2.24)$$

$$\langle m|\boldsymbol{a}\boldsymbol{a}^\dagger|n\rangle = (n+1)\langle m|n\rangle = (n+1)\,\delta_{m,n} \qquad (2.25)$$

$$\langle m|\boldsymbol{X}|n\rangle = \langle m|\frac{1}{\sqrt{2}}\left(\boldsymbol{a}^\dagger+\boldsymbol{a}\right)|n\rangle = \frac{1}{\sqrt{2}}\left(\sqrt{n+1}\,\delta_{m,n+1} + \sqrt{n}\,\delta_{m,n-1}\right) \qquad (2.26)$$

$$\langle m|\boldsymbol{P}|n\rangle = \langle m|\frac{j}{\sqrt{2}}\left(\boldsymbol{a}^\dagger-\boldsymbol{a}\right)|n\rangle = \frac{j}{\sqrt{2}}\left(\sqrt{n+1}\,\delta_{m,n+1} - \sqrt{n}\,\delta_{m,n-1}\right) \qquad (2.27)$$

$$\langle m|\boldsymbol{a}^2|n\rangle = \sqrt{n}\,\langle m|\boldsymbol{a}|n-1\rangle = \sqrt{n(n-1)}\,\langle m|n-2\rangle$$
$$= \sqrt{n(n-1)}\,\delta_{m,n-2} \qquad (2.28)$$

$$\langle m|\left(\boldsymbol{a}^\dagger\right)^2|n\rangle = \sqrt{n+1}\,\langle m|\boldsymbol{a}^\dagger|n+1\rangle = \sqrt{(n+1)(n+2)}\,\langle m|n+2\rangle$$
$$= \sqrt{(n+1)(n+2)}\,\delta_{m,n+2} \qquad (2.29)$$

Using the above results, the matrices for $\boldsymbol{a}$ and $\boldsymbol{a}^\dagger$ are shown below.

$$\boldsymbol{a} = \begin{bmatrix} 0 & \sqrt{1} & 0 & 0 & \cdots \\ 0 & 0 & \sqrt{2} & 0 & \cdots \\ 0 & 0 & 0 & \sqrt{3} & \cdots \\ \vdots & \vdots & \vdots & \vdots & \ddots \end{bmatrix} \quad \boldsymbol{a}^\dagger = \begin{bmatrix} 0 & 0 & 0 & \cdots \\ \sqrt{1} & 0 & 0 & \cdots \\ 0 & \sqrt{2} & 0 & \cdots \\ 0 & 0 & \sqrt{3} & \cdots \\ \vdots & \vdots & \vdots & \ddots \end{bmatrix} \qquad (2.30)$$

We can now use equations (2.5), (2.20) and (2.21) to determine the matrix elements of the Hamiltonian operator H as follows.

$$\langle m|\boldsymbol{X}^2|n\rangle = \langle m|\frac{1}{2}\left(\left(\boldsymbol{a}^\dagger\right)^2 + \boldsymbol{a}^\dagger\boldsymbol{a} + \boldsymbol{a}\boldsymbol{a}^\dagger + \boldsymbol{a}^2\right)|n\rangle$$

$$= \frac{1}{2}\left(\sqrt{(n+1)(n+2)}\,\delta_{m,n+2} + n\delta_{m,n} + (n+1)\delta_{m,n} + \sqrt{n(n-1)}\,\delta_{m,n-2}\right)$$

$$= \frac{1}{2}\left(\sqrt{(n+1)(n+2)}\,\delta_{m,n+2} + (2n+1)\delta_{m,n} + \sqrt{n(n-1)}\,\delta_{m,n-2}\right) \quad (2.31)$$

$$\langle m|\boldsymbol{P}^2|n\rangle = \langle m| -\frac{1}{2}\left(\left(\boldsymbol{a}^\dagger\right)^2 - \boldsymbol{a}^\dagger\boldsymbol{a} - \boldsymbol{a}\boldsymbol{a}^\dagger + \boldsymbol{a}^2\right)|n\rangle$$

$$= -\frac{1}{2}\left(\sqrt{(n+1)(n+2)}\,\delta_{m,n+2} - n\delta_{m,n} - (n+1)\delta_{m,n} + \sqrt{n(n-1)}\,\delta_{m,n-2}\right)$$

$$= -\frac{1}{2}\left(\sqrt{(n+1)(n+2)}\,\delta_{m,n+2} - (2n+1)\delta_{m,n} + \sqrt{n(n-1)}\,\delta_{m,n-2}\right)$$

$$= \frac{1}{2}\left(-\sqrt{(n+1)(n+2)}\,\delta_{m,n+2} + (2n+1)\delta_{m,n} - \sqrt{n(n-1)}\,\delta_{m,n-2}\right)$$

$$(2.32)$$

$$\langle m|\boldsymbol{H}|n\rangle = \langle m|\frac{\hbar\omega_0}{2}\left(\boldsymbol{X}^2 + \boldsymbol{P}^2\right)|n\rangle$$

$$= \frac{\hbar\omega_0}{4}\left(\sqrt{(n+1)(n+2)}\,\delta_{m,n+2} + (2n+1)\delta_{m,n} + \sqrt{n(n-1)}\,\delta_{m,n-2}\right)$$

$$+ \frac{\hbar\omega_0}{4}\left(-\sqrt{(n+1)(n+2)}\,\delta_{m,n+2} + (2n+1)\delta_{m,n} - \sqrt{n(n-1)}\,\delta_{m,n-2}\right)$$

$$(2.33)$$

∎

Chapter 3

Optical Implementations

In this chapter, we discuss optical implementations of quantum gates that were discussed in chapter 1. We will break up the quantum computation process into small pieces and realize these pieces using optical devices. We discuss the operations performed by these optical devices in detail. No familiarity is assumed with any of these devices.

3.1 What makes a good quantum computer?

In chapter 1, we discussed qubits and some commonly used single and multiple qubit gates. The biggest challenge in realizing quantum computation is that the requirements for feasible implementations are generally opposing: a quantum computer has to be isolated well enough to retain its quantum properties, but at the same time its qubits have to be accessible enough to be manipulated for computation. These two requirements are measured using what is known as "decoherence time" τ_Q, "operation time" τ_{op} and the "maximum number of operations" n_{op}. Various types of quantum systems have been proposed that attempt to find a good balance between these tradeoffs of quantum computation. Crude estimates of the properties of the most popular quantum systems can be found in [16] as shown in figure 3.1. Larger decoherence times usually indicate good isolation from the environment by means of fewer interactions with it, while smaller operation times imply faster unitary operations involving two or more qubits. The figure indicates the tradeoffs in the popular implementations of quantum computing.

Generally, the requirements for a good quantum computing scheme are the following [5]:

1. The scheme must have the ability to robustly represent quantum information

2. The scheme must have the ability to perform unitary transformations

3. The scheme must have the ability to prepare an initial state

4. The scheme must have the ability to measure the output result

System	τ_Q	τ_{op}	$n_{op} = \lambda^{-1}$
Nuclear spin	$10^{-2} - 10^8$	$10^{-3} - 10^{-6}$	$10^5 - 10^{14}$
Electron spin	10^{-3}	10^{-7}	10^4
Ion trap (In^+)	10^{-1}	10^{-14}	10^{13}
Electron $-$ Au	10^{-8}	10^{-14}	10^6
Electron $-$ GaAs	10^{-10}	10^{-13}	10^3
Quantum dot	10^{-6}	10^{-9}	10^3
Optical cavity	10^{-5}	10^{-14}	10^9
Microwave cavity	10^0	10^{-4}	10^4

Figure 3.1: Crude estimates of "decoherence time" τ_Q, "operation time" τ_{op} and "maximum number of operations" n_{op} for various implementations of quantum computing [16]. Note that $n_{op} = \lambda^{-1} = \tau_Q/\tau_{op}$.

In this chapter, we will discuss the optical implementation of quantum computing. We will realize some important quantum gates using optical devices and present the drawbacks to this scheme.

3.2   Optical devices for quantum computing

The optical photon is a chargeless particle that does not interact strongly with other particles or with its surrounding environment. For this reason, photons can be guided for very long distances with very little loss. Fiber optics is essentially an application of this feature of photons. In addition, photons can be delayed using phase shifters and combined using beamsplitters. In principle, photons can also be made to interact with each other by the use of non-linear media. We will consider Kerr media as our non-linear means of creating photon interactions.

Our method of approach will be as follows: we will first discuss quantum gates as applied to single and multiple qubits. Then, we will discuss the drawbacks of optical quantum computing and directions of current research.

Before discussing the quantum gates, we need to ask one important question. Assuming we have these quantum gates at our disposal, how do we create input and measure the output of our computation?

Photons will represent our qubits. While we could use polarization to form our computational basis, we will use two electromagnetic cavities with a total energy of $\hbar\omega$, which is a quantum or a photon. Because it is possible for a cavity to contain a superposition of zero or one photon, we have logical basis states from the cavity states related as shown below.

$$|\psi\rangle = c_0|0\rangle_L + c_1|1\rangle_L \equiv c_0|01\rangle + c_1|10\rangle \tag{3.1}$$

This is known as the *dual-rail* representation of the qubit [16]. Each cavity represents a different spatial mode.

We will generate single photons by attenuating the output of a laser. We will not discuss single photon generation in detail, but it suffices to mention that a laser outputs coherent states which can be attenuated to have just one photon with high probability. The interested reader is referred to [6] and [2] for popular techniques of single photon generation such as parametric down-conversion.

Measurement will be done using photon detectors. The interested reader is referred to [6] for an excellent discussion of photon detectors.

By taking the above features for granted, we have essentially satisfied the first, third and fourth requirements for a good quantum computing scheme as indicated on page 15. We will devote the rest of this chapter to the second requirement – that of performing unitary transformations.

3.3 Quantum gates using optical devices

Recall from equation (1.13) that we can decompose a unitary matrix into rotations and a global phase shift.

$$U = \exp\left(i\alpha\right) R_z(\beta) R_y(\gamma) R_z(\delta) \tag{3.2}$$

$$= e^{i\alpha} \begin{bmatrix} e^{-i\beta/2} & 0 \\ 0 & e^{i\beta/2} \end{bmatrix} \begin{bmatrix} \cos\frac{\gamma}{2} & -\sin\frac{\gamma}{2} \\ \sin\frac{\gamma}{2} & \cos\frac{\gamma}{2} \end{bmatrix} \begin{bmatrix} e^{-i\delta/2} & 0 \\ 0 & e^{i\delta/2} \end{bmatrix} \tag{3.3}$$

In optics, introducing phase shift can be achieved by devices known as retarders [9]. Our focus will be on the implementation of the other factors in the decomposition of a unitary matrix – the y and z rotations. Once we have these, we can realize single qubit gates. We will then introduce non-linearity using Kerr media to realize multiple qubit gates.

3.3.1 Single qubit gates

We have already mentioned that a retarder can introduce the global phase shift in the decomposition of a unitary matrix representing a single qubit operator. We begin by addressing the z rotation using a phase shifter.

A effect of a phase shifter is localized only to the modes going through it [14]. In other words, the effect of a phase shifter P can be described as follows.

$$P : |00\rangle \rightarrow |00\rangle \tag{3.4}$$

$$P : |01\rangle = a^\dagger|00\rangle \rightarrow |01\rangle \tag{3.5}$$

$$P : |10\rangle = b^\dagger|00\rangle \rightarrow e^{i\phi}|10\rangle \tag{3.6}$$

where ϕ is the phase shifter angle and $a^\dagger$ and $b^\dagger$ are the creation operators for the two modes representing the photon cavities. This phase shifter model acts on mode b only. Hence, a phase shifter leaves $|0\rangle_L$ unaffected and adds a phase shift to $|1\rangle_L$.

Its matrix representation is found as follows.

$$P : c_0|0\rangle_L + c_1|1\rangle_L \to c_0|0\rangle_L + c_1 e^{i\phi}|1\rangle_L \tag{3.7}$$

$$= e^{i\frac{\phi}{2}}\left(c_0 e^{-i\frac{\phi}{2}}|0\rangle_L + c_1 e^{i\frac{\phi}{2}}|1\rangle_L\right) \tag{3.8}$$

$$P \equiv e^{i\frac{\phi}{2}}\left[\begin{array}{cc} \exp\left(-i\phi/2\right) & 0 \\ 0 & \exp\left(i\phi/2\right) \end{array}\right] = e^{i\frac{\phi}{2}} R_z(\phi) \tag{3.9}$$

Hence, up to an irrelevant global phase, a phase shifter realizes rotation in the z axis. A phase shifter is simply drawn as a rectangle with the angle denoting the phase shift that it introduces. For the quantum-mechanically inclined, another way of looking at the phase shifter is its Hamiltonian below [16].

$$H_P = (n_0 - n)Z \tag{3.10}$$

$$P = \exp\left(-iH_P L/c_0\right) \tag{3.11}$$

In this notation, n_0 is the index of refraction of free space, n is the index of refraction of the phase shifter, Z is the Pauli-Z matrix, c_0 is the speed of light and L is the distance of propagation in the phase shifter.

Rotations about the y axis are realized using a beamsplitter. We will explain the effect of a beamsplitter B on different states below. Note that a beamsplitter is used to join states in different modes [14, 16].

$$B : |00\rangle \to |00\rangle \tag{3.12}$$

$$B : |0\rangle_L = |01\rangle = a^\dagger|00\rangle \to Ba^\dagger|00\rangle = Ba^\dagger B^\dagger B|00\rangle \tag{3.13}$$

$$= \left(a^\dagger \cos\theta + b^\dagger \sin\theta\right)|00\rangle = \cos\theta|01\rangle + \sin\theta|10\rangle \tag{3.14}$$

$$B : |1\rangle_L = |10\rangle = b^\dagger|00\rangle \to Bb^\dagger|00\rangle = Bb^\dagger B^\dagger B|00\rangle \tag{3.15}$$

$$= \left(-a^\dagger \sin\theta + b^\dagger \cos\theta\right)|00\rangle = -\sin\theta|01\rangle + \cos\theta|10\rangle \tag{3.16}$$

In the above equations, we have made use of two facts:

1. B is a unitary matrix. Hence, $BB^\dagger = B^\dagger B = I$ and

2. The expressions $Ba^\dagger B^\dagger$ and $Bb^\dagger B^\dagger$ are simplified using the Baker-Campbell-Hausdorf formula as shown in appendix C.

Hence, the matrix representation for B is derived as follows.

$$B : c_0|0\rangle_L + c_1|1\rangle_l \to c_0(\cos\theta - \sin\theta)|0\rangle_L + c_1(-\sin\theta + \cos\theta)|1\rangle_L \tag{3.17}$$

$$B \equiv \left[\begin{array}{cc} \cos\theta & -\sin\theta \\ \sin\theta & \cos\theta \end{array}\right] = e^{i\theta Y} = R_y(-2\theta) \tag{3.18}$$

Hence, a beamsplitter can be used to realize rotations in the y axis. There are several notations for a beamsplitter of angle θ. We present a beamsplitter and its adjoint in figure 3.2 with angle $\theta = \pi/4$. For the quantum-mechanically inclined, the
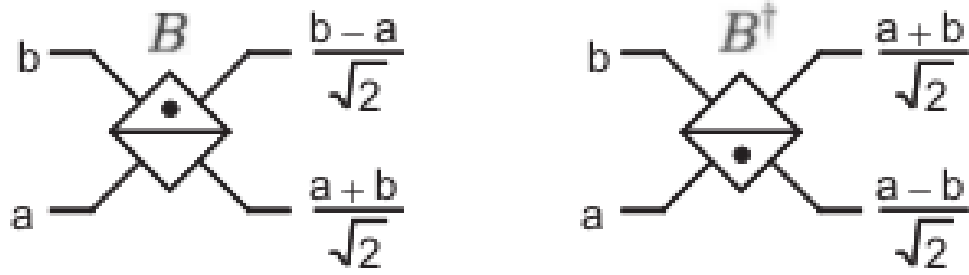
Figure 3.2: A beamsplitter and its adjoint acting on modes a and b for $\theta = \pi/4$.
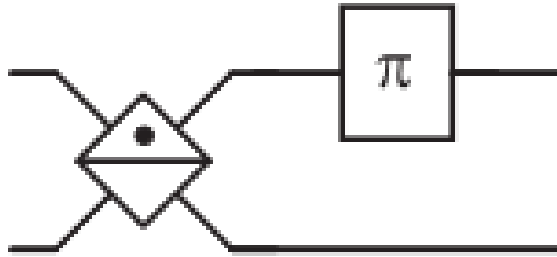

Figure 3.3: An optical implementation of the Hadamard gate

beamsplitter can also be defined with its Hamiltonian

$$H_B = i\theta \left(ab^\dagger - a^\dagger b \right) \tag{3.19}$$

$$B = \exp\left(iH_B \right) = \exp\left[\theta \left(a^\dagger b - ab^\dagger \right) \right] \tag{3.20}$$

where $a^\dagger$ and $b^\dagger$ are the creation operators of modes a and b respectively.

We have realized rotations in the y and z axes using phase shifters and beamsplitters without mentioning their physical implementations. Phase shifters are simply slabs of transparent media with indices of refraction that differ from that of air. Beamsplitters are partially silvered pieces of glass which reflect some of the incident light while transmitting the rest. For a beamsplitter of angle θ, $\cos\theta$ is the reflection coefficient and $1 - \cos\theta$ is the transmission coefficient.

3.3.2 The quantum Hadamard gate

In this section, we present the Hadamard gate as an example of a single qubit gate that can be realized by using a beamsplitter and a phase shifter together. Consider the circuit C in figure 3.3 with a 50-50 beamsplitter ($\theta = \pi/4$) and a phase shifter of angle π.

19

Its operation can be described based on our discussions above as follows.

$$C : |0\rangle_L \rightarrow \cos\theta |0\rangle_L + \sin\theta |1\rangle_L \tag{3.21}$$

$$C : |1\rangle_L \rightarrow -\sin\theta |0\rangle_L + \cos\theta |1\rangle_L \rightarrow \sin\theta |0\rangle_L - \cos\theta |1\rangle_L \tag{3.22}$$

$$C \equiv \begin{bmatrix} \cos\theta & \sin\theta \\ \sin\theta & -\cos\theta \end{bmatrix} = \frac{1}{\sqrt{2}} \begin{bmatrix} 1 & 1 \\ 1 & -1 \end{bmatrix} = H \tag{3.23}$$

Hence, the above circuit acts as a Hadamard gate. Note that the phase shifter only acts on the $|1\rangle_L$ mode. Several other optical circuits can be found in [16] and [14]. The latter uses slightly different notation than the one used here.

3.3.3 Multiple qubit gates

Now that we have realized single qubit gates, we focus our attention on multiple qubit gates. Without proof, we state here that single qubit gates and the CNOT gate form a universal set, i.e. we can make larger circuits that can be decomposed entirely into single qubit gates and controlled NOT gates [14]. Hence, our aim in this section is to discuss the optical implementation of the controlled NOT gate.

We begin by considering the index of refraction n of Kerr media.

$$n(I) = n + n_2 I \tag{3.24}$$

where I is the total intensity of light going through the medium. This is the optical Kerr effect. It is weakly seen in some commonly found materials such as glass. When two beams of light of equal intensity are co-propagated through a medium where the Kerr effect is visible, each beam experiences a phase shift directly proportional to the common intensity. This effect is not highly pronounced because of the usually small values of n_2. While one may attempt to increase the propagation distance to compensate for the small value of n_2, another challenge is faced: Kerr media are usually absorptive and scatter light out of its mode. For this reason, the methods we will now discuss are challenging to implement in a laboratory setting. Nevertheless, they provide the background required for other media in which the non-linear effect is more pronounced.

Kerr media provide cross phase modulation between two modes of light [16]. This is seen by the the Hamiltonian of a Kerr medium

$$H_K = -\chi a^\dagger a b^\dagger b \tag{3.25}$$

where a and b are the two modes of light and χ is the cross phase modulation which is dependent on n_2 in equation (3.24). The unitary operation of a Kerr medium is described by

$$K = e^{-iH_K L} = \exp\left(i\chi L a^\dagger a b^\dagger b\right) \tag{3.26}$$

where L is the distance of propagation. The effect of a Kerr medium on single photon states is described below:

$$K : |00\rangle \rightarrow |00\rangle \tag{3.27}$$
$$K : |01\rangle \rightarrow |01\rangle \tag{3.28}$$
$$K : |10\rangle \rightarrow |10\rangle \tag{3.29}$$
$$K : |11\rangle \rightarrow e^{i\chi L}|11\rangle \tag{3.30}$$

Setting $\chi L = \pi$, we have $K : |11\rangle \rightarrow -|11\rangle$.

Now consider a two-qubit system defined as follows:

$$|e_{00}\rangle \equiv |1001\rangle \tag{3.31}$$
$$|e_{01}\rangle \equiv |1010\rangle \tag{3.32}$$
$$|e_{10}\rangle \equiv |0101\rangle \tag{3.33}$$
$$|e_{11}\rangle \equiv |0110\rangle \tag{3.34}$$

If a Kerr medium is made to act on the two middle modes of this computational basis set, the following effects will be observed based on our description of Kerr media above.

$$K : |e_{00}\rangle \equiv |1001\rangle \rightarrow |1001\rangle \tag{3.35}$$
$$K : |e_{01}\rangle \equiv |1010\rangle \rightarrow |1010\rangle \tag{3.36}$$
$$K : |e_{10}\rangle \equiv |0101\rangle \rightarrow |0101\rangle \tag{3.37}$$
$$K : |e_{11}\rangle \equiv |0110\rangle \rightarrow -|0110\rangle \tag{3.38}$$

The Kerr medium acts only on the fourth basis state and leaves all other states as they are. The matrix representation of the Kerr medium shows this clearly.

$$K = \begin{bmatrix} 1 & 0 & 0 & 0 \\ 0 & 1 & 0 & 0 \\ 0 & 0 & 1 & 0 \\ 0 & 0 & 0 & -1 \end{bmatrix} \tag{3.39}$$

Note that the first two modes have been switched in the above computational basis set from the ones we have previously defined. This can be achieved physically using highly reflective mirrors.

This is a significant achievement, because the matrix representation of the controlled NOT gate can be written as follows.

$$U_{CN} = \underbrace{\frac{1}{\sqrt{2}}\begin{bmatrix} 1 & 1 & 0 & 0 \\ 1 & -1 & 0 & 0 \\ 0 & 0 & 1 & 1 \\ 0 & 0 & 1 & -1 \end{bmatrix}}_{I \otimes H} \underbrace{\begin{bmatrix} 1 & 0 & 0 & 0 \\ 0 & 1 & 0 & 0 \\ 0 & 0 & 1 & 0 \\ 0 & 0 & 0 & -1 \end{bmatrix}}_{K} \underbrace{\frac{1}{\sqrt{2}}\begin{bmatrix} 1 & 1 & 0 & 0 \\ 1 & -1 & 0 & 0 \\ 0 & 0 & 1 & 1 \\ 0 & 0 & 1 & -1 \end{bmatrix}}_{I \otimes H} \tag{3.40}$$

21

where $I \otimes H$ is the Hadamard gate which acts on the first two and last two modes separately. It is implemented using two sets of beamsplitters and phase shifters as seen in section 3.3.2. Note that we have set $\chi L = \pi$ for the Kerr medium. Hence, we have shown the theoretical realization of the controlled NOT gate using Kerr media, phase shifters and beamsplitters.

3.4　Drawbacks of the optical scheme

Our realization of quantum gates is theoretically complete. We generate photons using attenuated lasers and detect them using photodetectors [14, 16]. Single qubit gates can be realized using phase shifters and beam splitters, while multiple qubit gates can be realized using single qubit gates and the controlled NOT gate implemented by the cross phase modulation of Kerr media. So why hasn't a quantum computer been built yet?

We mentioned that an attractive feature of single photons for quantum computing is that they have minimal interaction with most matter. Unfortunately, photons do not interact among themselves as well. This implies that we will need to introduce non-linear effects such as the Kerr media discussed above. These non-linear effects introduce artifical interaction between the photons and fill the gap needed to realize quantum computing using single photons.

However, the best known Kerr media cannot produce cross phase modulation levels up to π. Even worse, an attempt to make up for the low cross phase modulation with a longer propagation distance results in absorption and scattering, which cause additional difficulties later on as we perform our measurements. This disadvantage becomes clear when we realize that approximately 50 photons will be absorbed for each photon cross modulated by an angle π [16].

Our study of single photon quantum computing is important because it reveals the features necessary for other implementations. Current research in the area of cavity quantum electrodynamics (cQED) is derived from the results learned in this scheme. In fact, one may think of the cQED scheme as single photon quantum computing with significantly better non-linear media.

Additionally, optical communication will also remain important in the years to come. While single photons may not be good candidates for a scalable quantum architecture, the energy required to transmit photons over optical fibers is significantly smaller than the energy required to transmit charges over a 50-ohm transmission line of the same distance. Therefore, single photon qubits may be essential for quantum communication rather than quantum computation. Active research on quantum communication channels and cryptography will soon reveal this. ∎

Chapter 4

Conclusion

In this thesis, we have achieved three objectives. First, we introduced the fundamental elements of quantum computation known as qubits. Then, we defined operations on individual qubits and discussed a universal set of operations that can be combined to form all others. We then showed operations that act on two qubits. The objective of this was to eventually find a universal set of operations consisting of single and multiple qubit gates that can be combined to form larger quantum circuits.

Next, we showed a quantum mechanical analysis of the harmonic oscillator as a preparation for following chapters. We discussed annihilator and creator operators in detail and determined the elements of their matrix representations.

Our next task was to realize these quantum gate operations. We discussed what makes a good quantum computer and showed some quantum computation schemes that have gained popularity through many years of research. We focused on the optical scheme in particular, and showed how to implement single qubit gates using retarders, beamsplitters and phase shifters. In order to realize multiple qubit gates, we introduced non-linearity through the use of Kerr media whose indices of refraction are related to the intensities of their inputs. We realized the controlled NOT gate using Kerr media and concluded by noting that single qubit gates and the controlled NOT gate form a universal set.

Finally, we dicussed the drawbacks of the optical scheme of quantum computation in preparation for further research on other schemes. We highlighted the weakness in our scheme resulting from the poor cross phase modulation of Kerr media and introduced cavity quantum electrodynamics as a scheme that attempts to solve this problem.

Our mathematical toolkit was strengthened with several figures and appendices that proved formulae used throughout the discussion.

Additional material on quantum computation can be found in [16]. The necessary background of quantum mechanics can be found in various sections throughout [8]. Optical implementations beyond the ones discussed here are given in a groundbreaking paper on linear optics quantum computing (LOQC) [14] and summarized in [15, 13, 12, 11]. General rules for physical implementations of quantum computation are given in [5]. The fundamentals of optics are discussed in [9] and expanded to quantum optics in [6]. The necessary background in linear algebra may be obtained from [18]. For

the mathematically inclined, [10, 3, 17] relate the mathematical ideas of quantum computing to Lie algebras.

Appendix A

Exponentiating Matrices

In this appendix, we prove the following.

$$\exp(iAx) = \cos(x)I + i\sin(x)A \tag{A.1}$$

for a real number x and matrix A such that $A^2 = I$ and $A^0 = I$. Recall the power series expansion for the exponential $\exp(x)$ for all x.

$$\exp(x) = \sum_{n=0}^{\infty} \frac{x^n}{n!} \tag{A.2}$$

We now rewrite this power series expansion for $\exp(x)$ after replacing x by iAx.

$$\exp(iAx) = \sum_{n=0}^{\infty} \frac{(iAx)^n}{n!} \tag{A.3}$$

$$= \frac{I}{0!} + \frac{iAx}{1!} + \frac{(iAx)^2}{2!} + \frac{(iAx)^3}{3!} + \ldots \tag{A.4}$$

$$= \frac{A^2}{0!} + \frac{iAx}{1!} + \frac{(iAx)^2}{2!} + \frac{(iAx)^3}{3!} + \ldots \tag{A.5}$$

Noting that even powers of A reduce to identity and $i^2 = -1$, we now rearrange the terms in the above equation as follows.

$$\exp(iAx) = \frac{A^2}{0!} + \frac{iAx}{1!} + \frac{(iAx)^2}{2!} + \frac{(iAx)^3}{3!} + \ldots \tag{A.6}$$

$$= \left(\frac{x^0}{0!} - \frac{x^2}{2!} + \frac{x^4}{4!} - \ldots \right) I + i \left(\frac{x^1}{1!} - \frac{x^3}{3!} + \frac{x^5}{5!} - \ldots \right) A \tag{A.7}$$

$$\tag{A.8}$$

The power series expansions for the sine and cosine functions appear in the above equation. We will state the power series expansions for these two functions below.

$$\sin x = \sum_{n=0}^{\infty} (-1)^n \frac{x^{2n+1}}{(2n+1)!} = \left(\frac{x^1}{1!} - \frac{x^3}{3!} + \frac{x^5}{5!} - \dots \right) \qquad (A.9)$$

$$\cos x = \sum_{n=0}^{\infty} (-1)^n \frac{x^{2n}}{(2n)!} = \left(\frac{x^0}{0!} - \frac{x^2}{2!} + \frac{x^4}{4!} - \dots \right) \qquad (A.10)$$

Therefore,

$$\exp(iAx) = \left(\frac{x^0}{0!} - \frac{x^2}{2!} + \frac{x^4}{4!} - \dots \right) I + i \left(\frac{x^1}{1!} - \frac{x^3}{3!} + \frac{x^5}{5!} - \dots \right) A \qquad (A.11)$$

$$= \cos(x)I + i\sin(x)A \quad \square \qquad (A.12)$$

Appendix B

Decomposing Unitary Matrices into Rotations

In this appendix, we prove that any unitary 2x2 matrix U can be decomposed into rotations as defined in (1.13), which we repeat here for convenience.

$$U = \exp\left(i\alpha\right) R_z(\beta) R_y(\gamma) R_z(\delta) \tag{B.1}$$

$$= e^{i\alpha} \begin{bmatrix} e^{-i\beta/2} & 0 \\ 0 & e^{i\beta/2} \end{bmatrix} \begin{bmatrix} \cos\frac{\gamma}{2} & -\sin\frac{\gamma}{2} \\ \sin\frac{\gamma}{2} & \cos\frac{\gamma}{2} \end{bmatrix} \begin{bmatrix} e^{-i\delta/2} & 0 \\ 0 & e^{i\delta/2} \end{bmatrix} \tag{B.2}$$

Consider the unitary matrix below. It is formed by carrying out the product above.

$$U = \begin{bmatrix} e^{i\left(\alpha-\frac{\beta}{2}-\frac{\delta}{2}\right)} \cos\frac{\gamma}{2} & -e^{i\left(\alpha-\frac{\beta}{2}+\frac{\delta}{2}\right)} \sin\frac{\gamma}{2} \\ e^{i\left(\alpha+\frac{\beta}{2}-\frac{\delta}{2}\right)} \sin\frac{\gamma}{2} & e^{i\left(\alpha+\frac{\beta}{2}+\frac{\delta}{2}\right)} \cos\frac{\gamma}{2} \end{bmatrix} \tag{B.3}$$

We claim that this is a unitary matrix for real numbers α, β, γ and δ. In order to prove this, we first find the adjoint of U, which is simply the conjugate transpose.

$$U^\dagger = \begin{bmatrix} e^{-i\left(\alpha-\frac{\beta}{2}-\frac{\delta}{2}\right)} \cos\frac{\gamma}{2} & e^{-i\left(\alpha+\frac{\beta}{2}-\frac{\delta}{2}\right)} \sin\frac{\gamma}{2} \\ -e^{-i\left(\alpha-\frac{\beta}{2}+\frac{\delta}{2}\right)} \sin\frac{\gamma}{2} & e^{-i\left(\alpha+\frac{\beta}{2}+\frac{\delta}{2}\right)} \cos\frac{\gamma}{2} \end{bmatrix} \tag{B.4}$$

Now, we compute $UU^\dagger$.

$$UU^\dagger = \begin{bmatrix} e^{i\left(\alpha-\frac{\beta}{2}-\frac{\delta}{2}\right)} \cos\frac{\gamma}{2} & -e^{i\left(\alpha-\frac{\beta}{2}+\frac{\delta}{2}\right)} \sin\frac{\gamma}{2} \\ e^{i\left(\alpha+\frac{\beta}{2}-\frac{\delta}{2}\right)} \sin\frac{\gamma}{2} & e^{i\left(\alpha+\frac{\beta}{2}+\frac{\delta}{2}\right)} \cos\frac{\gamma}{2} \end{bmatrix} \begin{bmatrix} e^{-i\left(\alpha-\frac{\beta}{2}-\frac{\delta}{2}\right)} \cos\frac{\gamma}{2} & e^{-i\left(\alpha+\frac{\beta}{2}-\frac{\delta}{2}\right)} \sin\frac{\gamma}{2} \\ -e^{-i\left(\alpha-\frac{\beta}{2}+\frac{\delta}{2}\right)} \sin\frac{\gamma}{2} & e^{-i\left(\alpha+\frac{\beta}{2}+\frac{\delta}{2}\right)} \cos\frac{\gamma}{2} \end{bmatrix} \tag{B.5}$$

$$= \begin{bmatrix} \cos^2\frac{\gamma}{2} + \sin^2\frac{\gamma}{2} & e^{-i\beta}\cos\frac{\gamma}{2}\sin\frac{\gamma}{2} - e^{-i\beta}\sin\frac{\gamma}{2}\cos\frac{\gamma}{2} \\ e^{i\beta}\sin\frac{\gamma}{2}\cos\frac{\gamma}{2} - e^{i\beta}\cos\frac{\gamma}{2}\sin\frac{\gamma}{2} & \sin^2\frac{\gamma}{2} + \cos^2\frac{\gamma}{2} \end{bmatrix} \tag{B.6}$$

$$= \begin{bmatrix} 1 & 0 \\ 0 & 1 \end{bmatrix} \tag{B.7}$$

$$= I \tag{B.8}$$

Hence, $UU^\dagger = I$. In other words, $U^\dagger = U^{-1}$. This is exactly the definition of a unitary matrix. Recalling that U was made up of the three smaller matrices with a global phase in (B.1) we have shown that any 2x2 unitary matrix can be written as a product of rotations in the z and y axes plus a global phase shift.

More generally, for two non-parallel real unit vectors $\hat{m}$ and $\hat{n}$, one may write

$$U = e^{i\alpha} R_{\hat{n}}(\beta) R_{\hat{m}}(\gamma) R_{\hat{n}}(\delta) \tag{B.9}$$

for some α, β, γ and δ.

Appendix C

The Baker-Campbell-Hausdorf Formula

The Baker-Campbell-Hausdorf formula for a complex number λ and operators A, G and C_n is given by

$$e^{\lambda G} A e^{-\lambda G} = \sum_{n=0}^{\infty} \frac{\lambda^n}{n!} C_n \tag{C.1}$$

where C_n is defined recursively such that $C_0 = A$ and $C_n = [G, C_{n-1}]$. Several references on Lie Algebras such as [10], [3] and [17] provide interesting proofs of the formula.

Here, we are interested in applying the Baker-Campbell-Hausdorf formula to the unitary matrix which represents the operation of an optical beamsplitter. In particular, for a beamsplitter B of angle θ, the unitary matrix representation is

$$B = \exp\left(\theta(a^\dagger b - a b^\dagger)\right) \tag{C.2}$$

For such a beamsplitter, we will compute $BaB^\dagger$ and $BbB^\dagger$ for annihilation operators a and b and creation operators $a^\dagger$ and $b^\dagger$. Recall from 2.2 that for annihilation operators α and β, $[\alpha, \alpha^\dagger] = [\beta, \beta^\dagger] = 1$ and $[\alpha, \beta] = [\alpha^\dagger, \beta] = [\alpha, \beta^\dagger] = [\alpha^\dagger, \beta^\dagger] = 0$. Setting G in (C.1) to $a^\dagger b - a b^\dagger$, we have

$$
\begin{aligned}
[G, a] &= (a^\dagger b - a b^\dagger) a - a(a^\dagger b - a b^\dagger) \\
&= a^\dagger b a - a b^\dagger a - a a^\dagger b + a a b^\dagger \\
&= a^\dagger b a - a a^\dagger b + a a b^\dagger - a b^\dagger a \\
&= [a^\dagger b, a] + a[a, b^\dagger]^{\,0} \\
&= [a^\dagger b, a] \\
&= a^\dagger b a - a^\dagger a b + a^\dagger a b - a a^\dagger b \\
&= a^\dagger [b, a]^{\,0} - [a, a^\dagger] b \\
&= -b
\end{aligned}
$$

29

Similarly, we can prove that $[G, b] = a$. We summarize these results below.

$$[G, a] = -b \tag{C.3}$$
$$[G, b] = a \tag{C.4}$$

We can now generalize the terms of C_n. Setting $C_0 = a$, $C_1 = [G, a] = -b$, $C_2 = [G, C_1] = -a$, $C_3 = [G, C_2] = b, \ldots$ and generally,

$$C_n = i^n a \text{ for even n}$$
$$C_n = i^{n+1} b \text{ for odd n}$$

Hence,

$$BaB^\dagger = e^{\theta G} a e^{-\theta G} \tag{C.5}$$

$$= \sum_{n=0}^{\infty} \frac{\theta^n}{n!} C_n \tag{C.6}$$

$$= \sum_{n=even} \frac{(i\theta)^n}{n!} a + i \sum_{n=odd}^{\infty} \frac{(i\theta)^n}{n!} b \tag{C.7}$$

$$= a \cos \theta + b \sin \theta \quad \square \tag{C.8}$$

Similarly,

$$Bb B^\dagger = -a \sin \theta + b \cos \theta \tag{C.9}$$
$$Ba^\dagger B^\dagger = a^\dagger \cos \theta + b^\dagger \sin \theta \tag{C.10}$$
$$Bb^\dagger B^\dagger = -a^\dagger \sin \theta + b^\dagger \cos \theta \tag{C.11}$$

Bibliography

[1] Simon Bone and Matias Castro. A Brief History of Quantum Computing. 1997.

[2] Gerard J. Milburn D. F. Walls. *Quantum Optics*. Springer, 2nd edition, 2008.

[3] Gustav W. Delius. Introduction to Quantum Lie Algebras. 1996.

[4] P.A.M. Dirac. *The Principles of Quantum Mechanics*. Oxford University Press, USA, 4th edition, 1982.

[5] David P. DiVincenzo. The Physical Implementation of Quantum Computation. 2000.

[6] Anthony Mark Fox. *Quantum Optics: An Introduction*. Oxford University Press, 1st edition, 2006.

[7] Herbert Goldstein, Charles P. Poole, and John Safko. *Classical Mechanics*. Addison Wesley, 3rd edition, 2001.

[8] David Griffiths. *Introduction to Quantum Mechanics*. Benjamin Cummings, 2nd edition, 2004.

[9] Eugene Hecht. *Optics*. Addison Wesley, 4th edition, 2001.

[10] James E. Humphreys. *Introduction to Lie Algebras and Representation Theory*. Springer-Verlag Berlin and Heidelberg GmbH & Co. K, 6th edition, 1997.

[11] E. Knill. Quantum gates using linear optics and postselection. *Phys. Rev. A*, 66:052306, Nov 2002.

[12] E. Knill, R. Laflamme, A. Ashikhmin, H. Barnum, L. Viola, and W. H. Zurek. Introduction to Quantum Error Correction. 2002.

[13] E. Knill, R. Laflamme, and G. Milburn. Thresholds for Linear Optics Quantum Computation. 2000.

[14] E. Knill, R. Laflamme, and G. J. Milburn. A scheme for efficient quantum computation with linear optics. *Nature*, 409, 2001.

[15] C. R. Myers and R. Laflamme. Linear Optics Quantum Computation: an Overview. 2005.

[16] Michael A. Nielsen and Isaac L. Chuang. *Quantum Computation and Quantum Information (Cambridge Series on Information and the Natural Sciences).* Cambridge University Press, 1st edition, 2004.

[17] A. Sagle and R. Walde. *Introduction to Lie Groups and Lie Algebras.* Academic Press, 1986.

[18] Gilbert Strang. *Introduction to Linear Algebra.* Wellesley Cambridge Press, 4th edition, 2009.